ORIGINAL PAPER

H.M. Sithole · P.E. Ngoepe · K. Wright

Atomistic simulation of the structure and elastic properties of pyrite (FeS$_2$) as a function of pressure

Abstract Interatomic potential parameters have been derived at simulated temperatures of 0 K and 300 K to model pyrite FeS$_2$. The predicted pyrite structures are within 1% of those determined experimentally, while the calculated bulk modulus is within 7%. The model is also able to simulate the properties of marcasite, even though no data for this phase were included in the fitting procedure. There is almost no difference in results obtained for pyrite using the two potential sets; however, when used to model FeS$_2$ marcasite, the potential fitted at 0 K performs better. The potentials have also been used to study the high-pressure behaviour of pyrite up to 44 GPa. The calculated equation of state gives good agreement with experiment and shows that the Fe–S bonds shorten more rapidly that the S–S dimer bonds. The behaviour of marcasite at high pressure is found to be similar to that of pyrite.

H.M. Sithole · P.E. Ngoepe
Materials Modelling Centre,
School of Physical and Mineral Sciences,
University of the North, P/Bag x 1106,
Sovenga 0727, South Africa

P.E. Ngoepe
Manufacturing and Materials Technology,
Council for the Scientific and Industrial Research,
PO Box 395, Pretoria 0002, South Africa

K. Wright (✉)
Departments of Chemistry and Earth Sciences,
University College London, Gower Street,
London WC1 E 6BT, UK

K. Wright
Royal Institution, Albemarle Street,
London W1 S 4BS, UK
e-mail: kate@ri.ac.uk
Fax: +44-207-670-2920

Present address H.M. Sithole
De Beers Consolidated Mines,
TSS Technologies, PO Box 82851, Southdale,
Johannesburg, South Africa

Introduction

Pyrite (FeS$_2$) is the most abundant iron sulphide mineral in nature and is found in a wide range of geological environments. Its crystal structure is based on that of NaCl, with the anions replaced by S$_2$ dimers whose axes are oriented along the four {111} cube directions. Each Fe atom is coordinated by six sulphurs in a slightly distorted octahedron, and each S is tetrahedrally coordinated to three Fe atoms and its dimer pair. The pyrite group of minerals includes CoS$_2$, NiS$_2$, CuS$_2$ and ZnS$_2$, all of which have very different electrical and magnetic properties (Bullett 1982). For example, CoS$_2$ is a ferromagnetic metal, NiS$_2$ a paramagnetic Mott–Hubbard insulator, CuS$_2$ a (metallic) superconductor and ZnS$_2$ a diamagnetic insulator. Thus they attract a great deal of interest from both physicists and mineralogists, and offer a challenging group of minerals for the study of physical properties and electronic structure using both experimental and theoretical methods.

The electronic, structural and physical properties of pyrite have been extensively investigated using a variety of spectroscopic methods. It is a diamagnetic semiconductor with an experimentally determined band gap of ~0.95 eV (Li et al. 1974; Vaughan 1985). Hence, the octahedrally coordinated Fe^{2+} in pyrite is in a low-spin state with an electronic configuration of $(t_{2g})^6$ $(e_g)^0$. (Tossell and Vaughan 1992). Mössbauer studies (Finklea et al. 1976) have confirmed that Fe is present in the Fe^{2+} state. A range of computational studies using methods based on density functional theory (DFT) (e.g. Zhao et al. 1993; Raybaud et al. 1997; Eyert et al. 1998; Sithole et al. 1999) and Hartree–Fock (HF) (Muscat et al. 2002) have also been employed to study the electronic structure of pyrite and related minerals, with varying results. Calculated band gaps range from 0.3 eV (Zeng and Holzworth 1994) to 11.0 eV (Muscat et al. 2002), depending on the type of method used.

The structure of pyrite under ambient conditions is well known, although reported lattice parameters range from 5.406 Å (Straumanis et al. 1964) to 5.428 Å (Finklea et al. 1976), probably due to the presence of impurities or point defects such as vacancies (Birkholz et al. 1991). The cubic structure is thought to remain stable up to very high pressures, and this is certainly the case up to almost 50 GPa (Merkel et al. 2002). Measurements of the elastic properties of pyrite have been carried out over a range of pressure conditions up to 48 GPa, and reported bulk moduli (K_0) range from 133.5 GPa (Merkel et al. 2002) to 155 GPa (Benbattouche et al. 1989). This variation has recently been attributed to differences in experimental setup and to sample stress conditions (Merkel et al. 2002), although the defect structure and impurity content may also affect the compressibility. Ab initio calculations have been performed to establish the zero pressure properties of pyrite, but tend to overestimate its elastic stiffness, giving K_0 values in the range 165 GPa (Sithole et al. 1999) to 675 GPa (Temmerman et al. 1993).

In the present work, interatomic potentials, based on classical mechanics, are derived and used to model the elastic behaviour of pyrite over a range of pressure conditions. This type of approach has the advantage that it requires minimal computational resources while providing information on those properties that do not rely directly on the electronic structure. This work complements earlier studies of pyrite elasticity while at the same time providing a rigorous test of the methodology and the potential parameters used. In the following sections we briefly describe the procedure for deriving interatomic potential parameters to model pyrite, and present the calculated structure as well as the elastic constants as a function of pressure. In order to test our model further, we have calculated the structure and high pressure behaviour of marcasite, the metastable polymorph of FeS_2.

Theoretical methods

Theoretical studies of materials require a model of the forces acting between the atoms in a solid. The atomistic simulation method uses interatomic potential functions to describe the total energy of a system in terms of atomic coordinates. Thus the equilibrium positions of atoms or ions in a system are evaluated by minimizing the lattice energy until all strains acting on the crystal are removed. The lattice energy can be defined as the sum of the electrostatic or Coulombic forces acting between atoms, and the short-range repulsive forces produced by the overlap of nearest-neighbour electron clouds and Van der Waals forces. These short-range forces act between bonded and non-bonded atoms in the crystal, where non-bonded interactions can be effectively modelled by the Buckingham potential:

$$U_{ij}^{Buck} = A_{ij} \exp -(r_{ij}/\rho_{ij}) - C_{ij}r_{ij}^{-6} \qquad (1)$$

The parameters A_{ij} and ρ_{ij} describe the repulsion between two ions i and j at a separation distance r_{ij}, and C_{ij} is a term included to model dispersion. Bonded interactions can be described by a combination of two-body bond-stretching potentials, such as a harmonic potential of the form:

$$U_{ij}^{Harm} = 0.5k_s(r_{ij} - r_0)^2 \ , \qquad (2)$$

Three-body bond-bending terms that are exponentially decaying, can be used to include the effects of directionality in S–S–Fe bonds.

$$U_{jik}^{b} = 0.5k_b(\theta_{jik} - \theta_0)^2 \exp (r_{ij}/\rho_1) \exp (-r_{jk}/\rho_2) \ . \qquad (3)$$

In (2) and (3) k_s and k_b are the bond-stretching and bond-bending force constants, respectively, and θ_0 the equilibrium bond angle.

The short-range potential parameters used to describe interactions in pyrite were derived by a least-squares fitting procedure using the GULP code (Gale 1997). The fit was performed using the experimentally determined crystal structure of Brostigen and Kjekshus (1969) and the zero pressure elastic constants of Benbattouche et al. (1989) with the charges fixed at Fe^{2+} and S^-. Interactions between the S atoms within the dimer are modelled by a harmonic function (Eq. 2) with a cut-off of 2.5 Å, while all other two-body terms are described by a Buckingham term whose cutoff is set to 12 Å. The potential parameters were varied until the differences between calculated and experimental structure and properties were minimized. In general, fitted parameters are derived for implicit temperature, which ignores the fact that the experimental data were obtained at a finite temperature. However, the fit can also be carried out with the explicit inclusion of temperature. In this study, we have derived two sets of potentials, in order to compare implicit and explicit temperature effects. All calculations at finite temperature were performed using free energy minimization within the quasiharmonic approximation, with a k-point grid of $8 \times 8 \times 8$, which gave convergence of the energy to better than 0.0001 eV. Minimization was carried out only with respect to the unit-cell coordinates (ZSISA).

The fitting procedure was first carried out at 0 K (P1), then at a simulated temperature of 300 K (P2). In both cases a relaxed fitting procedure was adopted where the structure is optimized at each stage of the fit and compared to the experimental structure. Thus, the fit directly minimizes atomic displacements rather than forces (see Gale 1996 for further details). Several attempts were made to integrate the effects of polarizability on the S ion by the use of a shell model (Dick and Overhauser 1958). However, adding this term did not lead to an improvement in the model and thus was not included.

Results and discussion

Potential model and zero-pressure properties

Evidence from experiments (Finklea et al. 1976) and from ab initio calculations (Sithole 2000) suggests that bonding between the S–S dimer pair in pyrite is likely to be largely covalent, with a more mixed character for the Fe–S interaction. Therefore both bonded and non-bonded interactions were included in the potential parameter set to reproduce the structure and properties of pyrite, as well as three-body bending terms that simulate the directionality of the bonds. The interatomic potential parameters derived at 0 K (P1) and 300 K (P2) are given in Table 1, while the calculated structural and elastic properties are compared to the experimental values in Table 2. Potential P1 incorporates a Buckingham term for Fe–Fe interactions, which is absent in P2. This is offset in P2 by the large A value in the S–S and S–Fe Buckingham terms. It can readily be seen from Table 2 that both potentials perform well at 0 and 300 K and reproduce the cell parameter, bond lengths and bond angles to within 1% of the measured values. The calculated elastic properties of pyrite are within 5% of experiment for P1, and 7% for P2. Given the

Table 1 Potential parameters for pyrite fitted at 0 K (P1) and 300 K (P2)

	P1			P2		
Buckingham	A(eV)	ρ (Å)	C(eV Å^6)	A(eV)	ρ(Å)	C(eV Å^6)
S–S	625.17	0.3308	96.357	3435.7274	0.298280	121.78
Fe–S	29451.7108	0.200259	0.0	58368.1313	0.1899	0.00
Fe–Fe	36224.847	0.3000	0.0	0.0	0.0	0.00
Harmonic	K_s(eV Å^{-2})	r_0(Å)		K_s(eV Å^{-2})	r_0(Å)	
S–S	6.585968	2.5249		5.61798	2.563455	
Three-body	K_b (eV rad^2)	θ_0°		K_b (eV/rad^2)	θ_0°	
S–Fe–S	664386.6233	105.485		960312.0637	102.103	

Table 2 Comparison of the calculated and experimental structure and elastic properties of pyrite (FeS$_2$). (Structure data from Brostigen and Kjekshus (1969), elastic data from Benbattouche et al. 1989)

Parameter	P1 (0 K)	P1 (300 K)	P2 (0 K)	P2 (300 K)	Expt
a (Å)	5.408	5.431	5.374	5.379	5.418
Vol (Å^3)	158.186	160.227	155.257	155.668	159.05
Distances (Å)					
S–S	2.171	2.179	2.168	2.174	2.177
Fe–S	2.258	2.269	2.243	2.245	2.262
Fe–Fe	3.824	3.842	3.800	3.804	3.831
Elastic constants (GPa)					
C_{11}	373.64	352.56	386.9	387.51	366.0
C_{12}	48.61	47.91	44.4	44.84	47.0
C_{44}	103.95	101.74	105.6	106.75	105.0
K	157	149.47	158.00	159.06	155

approximate nature of the model, the agreement is extremely good in both cases.

In order to test the models further, and to gauge their transferability, we used them to calculate the structure and properties of the metastable polymorph of FeS$_2$, marcasite (Table 3). No data on this material were included in the fitting procedure. The structure of marcasite is orthorhombic and, energetically, the difference between the two polymorphs is small. Pyrite is more stable than marcasite by around 3.9 kJ mol^{-1} at room temperature (Lennie and Vaughan 1992). Using potential P1, the predicted cell parameters of marcasite are shortened along a and elongated along c, with the overall cell volume being within 0.5% of the experimental value. P2 performs slightly better, although the change in cell volume is about the same as P1. Both P1 and P2 show a value of b consistent with experiment. The calculated total energy difference between pyrite

Table 3 Comparison of the calculated (0 K) and experimental structure and elastic properties of marcasite (FeS$_2$). (Structure data from Kjekshus and Rakke 1975)

Parameter	P1	P2	Expt
a (Å)	4.121	4.177	4.436
b	5.414	5.414	5.414
c	3.625	3.537	3.381
c/a	0.879	0.847	0.762
Vol (Å^3)	80.936	80.418	81.199
Distances (Å)			
S–S	2.107	2.248	2.212
Fe–S	2.233	2.219	2.230
Fe–Fe	3.625	3.537	3.831
Bulk modulus (GPa)	152.22	163.06	

and marcasite gives the correct order of stability with values of 3.4 kJ mol^{-1} using P1, which is very close to that found by experiment, and 46.0 kJ mol^{-1} with P2. No experimental information on bulk modulus is available for marcasite, however, our calculated values are similar to those determined for pyrite, which, on the basis of quantum-mechanical calculations (Sithole 2000), is what we would expect.

Pyrite and, to a lesser extent, marcasite, have been the subject of numerous ab initio studies aimed at understanding the electronic structure. Reported cell parameters for pyrite range from 6.0 Å using HF (Muscat et al. 2002), to 5.299 Å obtained with DFT (Raybaud et al. 1997). Values of bulk modulus (K) also vary depending on the computational method employed. For example, Sithole et al. (1999) obtain $K = 184$ GPa using the planewave pseudopotential method, and 165 GPa with a full potential linear muffin tin orbital (FP-LMTO) approach. This is similar to the value of 164 GPa reported by Muscat et al. (2002). All the above methods give bulk moduli larger than those reported from experiment, even allowing for the spread of the measured data. Sithole (2000) has also calculated K for marcasite using DFT, which was predicted to be 181 GPa. Therefore we would expect the bulk modulus of marcasite to be close to that of pyrite.

Effects of pressure

The discussion above shows that our potentials are able to accurately simulate the 0 GPa pressure structure and elastic properties of pyrite and of marcasite. Thus we can have some confidence that they will also give a good
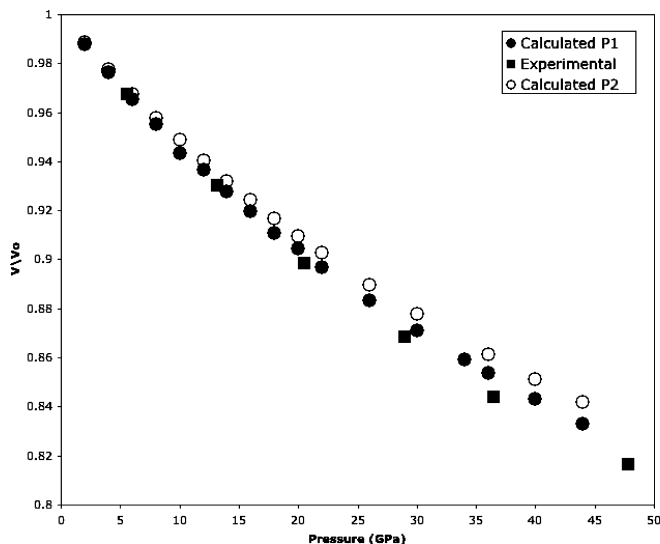
Fig. 1 The calculated EOS for pyrite using P1 and P2, and the experimental data of Merkel et al. (2002) for comparison

Fig. 2 The change in Fe–S (*squares*) and S–S (*diamonds*) bond lengths as a function of increasing pressure. P1 *filled symbols*; P2 *open symbols*

Fig. 3 Variation of the elastic constants of pyrite with increasing pressure, calculated using potential P1

description of these properties at higher pressures. The effect of pressure on the structure and on the elastic constants of pyrite was calculated up to simulated pressures of 44 GPa using potentials P1 and P2. The variation in volume as a function of pressure as calculated by the two potentials is compared with the experimental values of Merkel et al. (2002) in Fig. 1. The predicted equation of state (EOS) closely follows the experimental EOS, although there is a slight deviation at higher pressures. For P1, the cell volume changes by 16.69% from 158.28 to 131.86 Å^3 over the pressure range 0–44 GPa. Using P2, the volume change is slightly smaller, 15.83%, with the initial and final volumes being 153.69 and 129.36 Å^3, respectively. Bond lengths for Fe–S are predicted to shorten much more slowly than those of the S–S dimer pair as shown in Fig. 2, although in both cases the actual change is linear with increasing pressure. This behaviour was also predicted by the TB-LMTO calculations of Sithole et al. (1999). Similarly, we find that the elastic constants (Fig. 3) increase smoothly as a function of pressure, with C_{11} increasing more sharply than C_{12} and C_{44}.

Only limited data are available on the response of the structure and elasticity of pyrite at high pressure. The experimental work of Clendenen and Drickamer (1966) measures the change in volume of pyrite up to 28.5 GPa, The pressure dependence of the bulk modulus and elastic constants was determined by Benbattouche et al. (1989) to 0.15 GPa and more recently by Merkel et al. (2002) to 48.5 GPa. The results of our calculations closely follow the experimental trends and are quantitatively the same to within a few percent. We are therefore confident that our potentials are able to accurately simulate the properties of pyrite at high pressure.

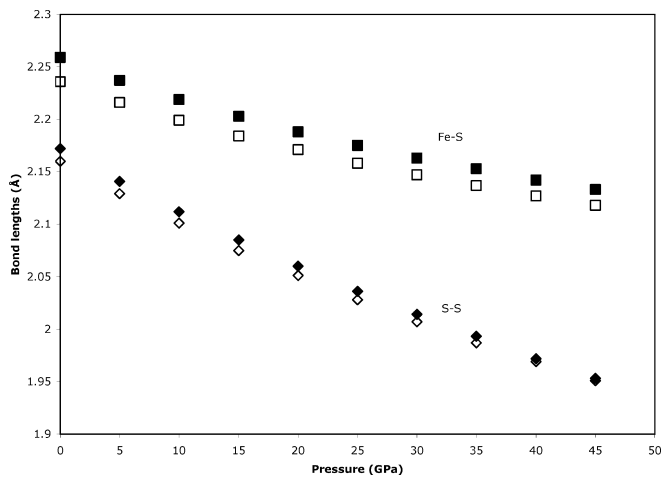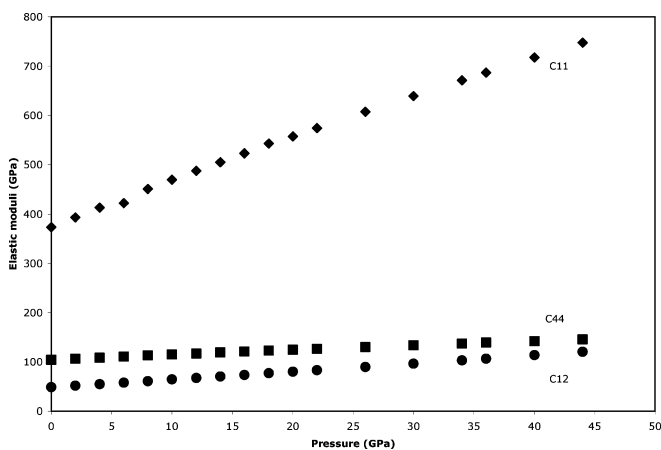We now turn to the high-pressure behaviour of marcasite, for which no experimental data are available.

The EOS of marcasite is compared to that of pyrite in Fig. 4, which shows that both phases behave in a very similar manner. The marcasite unit cell shortens by 9.4% along *a* over the pressure range 0–44 GPa, 6% along *b*, but only 3.3% along *c*. In pyrite, the S–S and Fe–S distances shorten by 10% and 5.5%, respectively, almost the same as the 11 and 5% for the same bonds in marcasite. Energetically, the difference between the two phases becomes more pronounced with pyrite being more stable than marcasite by almost 20 kJ mol^{-1} at 44 GPa.

Conclusions

Despite its apparently covalent nature, it has been possible to derive classical ionic interatomic potential models with which to describe pyrite. This type of approach is less rigorous than those based on quantum mechanics as it use a number of approximations.
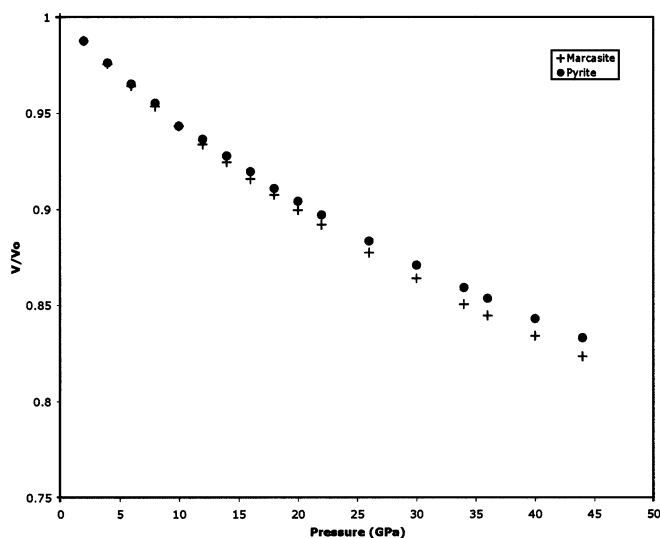
Fig. 4 EOS of marcasite and pyrite calculated with P1

However, it has the advantage that it can be used routinely to investigate structures and properties over a range of pressure and temperature conditions. The quality of the potentials is good, as shown by the agreement between calculated and experimental ambient pressure structure and elastic properties of pyrite. In addition, the ability of the models to simulate the structure of marcasite, even though no data for marcasite were included in the fitting procedure, indicates that we are correctly describing the Fe–S interaction. The high-pressure structural properties and elastic constants compare well with experimental results and predict that marcasite will react in a manner similar to pyrite when compressed.

The usefulness of performing the fitting procedure at a simulated temperature of 300 K, i.e. with the explicit inclusion of temperature, appears to be limited, since the results do not differ greatly. However, this may not be the case when modelling variations in temperature. An examination of the high-temperature properties of pyrite is currently underway and will be reported in detail in a separate paper.

References

Benbattouche N, Saunders GA, Lambson EF, Hölne W (1989) The dependences of the elastic stiffness moduli and the Poisson ratio of natural iron pyrites (FeS$_2$) upon pressure and temperature. J Phys (D) Appl Phys 22: 670–675

Birkholz M, Fiechter S, Hartmann A, Tributsch H (1991) Sulfur deficiency in iron pyrite (FeS$_{2-x}$) and its consequences for band structure models. Phys Rev (B) 43: 11926–119236

Brostigen G, Kjekshus A (1969) Redetermined crystal structure of FeS$_2$ (pyrite) Acta Chem Scand 23: 2186–2188

Bullett DW (1982) Electronic structure of 3d pyrite- and marcasite-type sulphides. J Phys (C) Solid State Phys 15: 6163–6174

Clendenen RL, Drickamer (1966) Lattice parameters of nine oxides and sulfides as a function of pressure. J Chem Phys 44: 4223–4228

Dick BG, Overhauser AW (1958) Theory of the dielectric constants of alkali halide crystals. Phys Rev 112: 90–103

Eyert V, Höck K-H, Fiechter S, Tributsch H (1998) Electronic structure of FeS$_2$: the crucial role of electro-lattice interaction. Phys Rev (B) 57: 6350–6359

Finklea SL, Cathey LC, Amma EL (1976) Investigation of the bonding mechanism in pyrite using the mössbauer effect and X-ray crystallography. Acta Crystallogr (A) 32: 529–537

Gale JD (1996) Empirical potential derivation for ionic materials. Philos Mag 73: 3–19

Gale JD (1997) GULP: a computer program for the symmetry-adapted simulation of solids. J Chem Soc, Faraday Trans, 93: 629–637

Kjekshus A, Rakke T (1975) Compounds with the marcasite type crystal structure. XI. High-temperature studies of chalcogenides. Acta Chem Scand (A) 29: 443–452

Lennie AR, Vaughan DJ (1992) Kinetics of the marcasite–pyrite transformation: an infrared spectroscopic study. Am Mineral 77: 1166–1171

Li RK, Johnson KH, Eastman DE, Freeouf JL (1974) Localized and band-like electron states in FeS$_2$ and NiS$_2$. Phys Rev Lett 32: 470–472

Merkel S, Jephcoat AP, Shu J, Mao H-K, Gillet P, Hemley RJ (2002) Equation of state, elasticity and shear strength of pyrite under high pressure. Phys Chem Miner 29: 1–9

Muscat J, Hung A, Russo S, Yavrovsky I (2002) First-principles study of the structural and electronic properties of pyrite FeS$_2$. Phys Rev (B) 65 054107

Opahle L, Koepernik K, Eschrig, H (1999) Full potential band-structure calculations of iron pyrite. Phys Rev (B) 60: 14035–14041

Raybaud P, Kresse G, Hafner J, Toulhoat H (1997) Ab initio density functional studies of transition-metal sulphides: I. Crystal structure and cohesive properties. J Phys Condens Matter 9: 11085–11106

Sithole HM (2000) Electronic and atomistic simulation of iron sulfides. PhD Thesis, University of the North, South Africa

Sithole HM, Nguyen-Manh D, Pettifor DG, Ngoepe PE (1999) Internal relaxations, band gap s and elastic constant calculations of FeS$_2$. Mol Sim 22: 31–37

Straumanis ME, Amstutz GC, Chan S (1964) Lattice parameters and expansion coefficients of FeS$_2$ (natural and synthetic), and of CoS$_2$. Am Mineral 49: 206–212

Temmerman WM, Durham PJ, Vaughan DJ (1993) The electronic structures of the pyrite-type disulphides (MS$_2$, where M = Mn, Fe, Co, Ni, Cu, Zn) and the bulk properties of pyrite from local density approximation (LDA) band structure calculations. Phys Chem Miner 20: 248–254

Tossell JA, Vaughan DJ (1992) Theoretical geochemistry. Applications of quantum mechanics in the Earth and mineral sciences OUP, New York

Vaughan DJ (1985) Spectroscopy and chemical bonding in the opaque minerals. In: Berry FJ, Vaughan DJ (eds) Chemical bonding and spectroscopy in mineral chemistry. Chapman and Hall, London

Zeng Y, Holzwarth NAW (1994) Density-functional calculation of the electronic structure and equilibrium geometry of iron pyrite (FeS$_2$) Phys Rev (B) 50: 8214–8220

Zhao GL, Callaway J, Hayashibara M (1993) Electronic structure of iron and cobalt pyrites. Phys Rev (B) 48: 15781–15786